Atomic and electronic structure of WSe_2 from *ab initio* theory: Bulk crystal and thin film systems

D. Voß, P. Krüger, A. Mazur, and J. Pollmann
Institut für Theoretische Physik II - Festkörperphysik, Universität Münster, D-48149 Münster, Germany
(Received 7 July 1999)

We report on *ab initio* bulk and surface atomic and electronic structure calculations of WSe_2. The calculations are based on the local-density approximation employing nonlocal, normconserving pseudopotentials together with Gaussian orbital basis sets. We have carried out a fairly general case study including analyses of the effects of basis set, **k** integration, structure parameters, and relativistic corrections on the band structure and the atomic properties. We find that the energy of particular band-edge states is extremely sensitive with respect to the lattice parameters and to spin-orbit coupling. Our results for the bulk atomic and electronic structure resolve recent controversies in these quantities, as discussed in the literature, and shed light on their origins. In particular, it had been suggested that surface effects might be the cause of the deviations. To resolve this issue, we have studied surface atomic and electronic properties for a number of WSe_2 thin films. Our results allow us to quantitatively interpret experimental results from angle-resolved photoemission spectroscopy and to predict the influence of the film thickness on electronic properties. [S0163-1829(99)04843-2]

I. INTRODUCTION

Within the last decade the properties of many layered transition-metal dichalcogenides have been investigated in detail. WSe_2, which belongs to this group of materials, is a semiconductor with a fundamental band gap of 1.2 eV. It consists of sandwich layers of about 3.3 Å thickness comprising a metal layer in the middle and two chalcogen layers, one above and one below the metal layer. These sandwich layers are separated from each other by 3.1 Å giving rise to the layered structure of the material. There is a strong *p-d* interaction within the layers but only a fairly weak van der Waals interaction between neighboring sandwich layers. The bulk crystal, in consequence, shows significant anisotropy effects in relevant physical properties. These can be used to open up a wide range of possible applications. The physical properties of layered transition-metal dichalcogenides can, e.g., be monitored in the laboratory by intercalating layers of other materials between the sandwiches giving rise to largely different properties, as one example.

Furthermore, there are very interesting possibilities of creating microscopic structures by manipulating a WSe_2 surface on a *nm* scale or even on an atomic scale by the tip of a scanning tunneling microscope (STM).[1,2] The creation of such structures of *nm* size can be achieved by the variation of the tip distance from the sample surface, as well as, by applying voltage pulses.[3,4] The resulting structures, which appear as hills with a diameter of a few *nm*, were found to be time-stable when their creation was achieved by voltage pulses. Besides, they could be erased in a well-defined way.[3]

In addition, the size of the gap and the high resistance against photocorrosion makes this material interesting for photovoltaic applications. Indeed, WSe_2 is known as a prototype for electrochemical solar cells.[5,6] Efficiencies up to 17.1% for an n-$WSe_2/I^-,I_2/Pt$ solar cell have been reported.[7] In this context, the electronic structure of WSe_2, in general, and the exact position of its valence-band maximum (VBM) in **k** space, in particular, have been subject of a number of detailed experimental and theoretical investigations.[8–11] Straub *et al.*[8] and Finteis *et al.*[9] have compared their angle-resolved photoelectron spectroscopy (ARPES) and angle-resolved inverse photoelectron spectroscopy (ARIPES) data with the results of their full potential fully relativistic linear augmented plane-wave (LAPW) calculations. Traving *et al.*[11] compared their ARPES and ARIPES data with the results of their fully relativistic linear muffin-tin orbital (RLMTO) and extended linear augmented plane-wave (ELAPW) calculations. While the latter authors[11] find the VBM near the Γ point, the former authors[8,9] find it near the sixfold degenerate K point. In the detailed results of these references[8,9,11] there are more subtle deviations, in addition. The partially controversial results of these publications[8,9,11] have been vividly discussed during the last few years.

Very recently, Finteis *et al.*[10] have reported in an ERRATUM, that their finding concerning the type of the band gap (direct versus indirect) originated from an incorrect structure parameter used in their calculations (c value, see below). Still, there are differences in the results of the two different approaches, cited above. There remain questions with respect to the basis set, the potential, the self-consistency procedure, the lattice constants, and the importance of relativistic corrections.

To contribute to a more basic understanding of important physical properties of transition-metal dichalcogenides, in general, and of WSe_2, in particular, we have carried out a systematic *ab initio* case study of the atomic and electronic structure of WSe_2, investigating the influence of calculational details (basis set, pseudopotentials, scalar or fully relativistic calculations, experimental or theoretical lattice constants) on the resulting properties. By applying these approaches within the same methodological framework, we can identify which features in the results are mere artifacts of the approximation used and which are true physical properties of WSe_2.

In addition, we have thoroughly investigated the buildup of the bulk band structure with the number of sandwich layers. For this purpose, we have investigated films of one up to five sandwich layers (i.e., three up to fifteen atomic layers). In particular, the five sandwich system can be regarded as a model of the experimentally investigated surface systems.

The paper is organized as follows. In Sec. II, we briefly describe the theoretical method applied. Setion. III is devoted to the presentation and discussion of our theoretical results. Structural and electronic properties of the WSe_2 *bulk* crystal are discussed in Sec. III in comparison with ARPES and ARIPES data from experiment. In Sec. III A, we report structural and electronic properties of thin WSe_2 *films* of varying thickness in comparison with respective data. A short summary concludes the paper in Sec. IV.

II. METHOD OF CALCULATION

The calculations have been carried out employing density functional theory within local-density approximation (LDA).[12] We have used the normconserving, nonlocal pseudopotentials of Bachelet, Hamann, and Schlüter[13] in the nonseparable form of Ref. 13, as well as, normconserving, nonlocal pseudopotentials of Gonze, Stumpf, and Scheffler[14] in the fully separable form of Kleinman and Bylander.[15] The exchange-correlation energy was taken into account using the Ceperley-Alder[16] form as parametrized by Perdew and Zunger.[17]

As a basis to represent the wave functions, we use 100 Gaussian orbitals of *s*, *p*, *d*, and *s** symmetry per sandwich layer and spin. Since two sandwich layers are contained in the bulk unit cell, we employ 200 localized orbitals in our basis for a *bulk* calculation. These orbitals are localized at the atomic positions, namely 40 at each W and 30 at each Se atom. As decay constants of the Gaussians we employ 0.17, 0.45, 1.18, and 3.10 for tungsten and 0.17, 0.41, 1.00 for selenium (in atomic units). A linear mesh of about 0.2 Å in real space is used for the representation of the charge density and the potential. Test calculations with an extended basis set including Gaussians that are localized between the sandwich layers, as well as, denser meshes exhibit only negligible changes in the electronic properties. The spin-orbit interaction is considered in each step of the iteration. It is treated in an on-site approximation, i.e., only integrals with the same location of the Gaussian orbitals and the spin-orbit potential are taken into account. In our calculations of the properties of WSe_2 *films* we have employed supercells of one up to five sandwich layers separated by appropriately thick vacuum layers. Brillouin-zone integrations in the *bulk* calculations have been carried out using 12 special **k** points in the irreducible part while in our *thin film* calculations we have used 6 special **k** points.

III. RESULTS AND DISCUSSION

WSe_2 consists of single Se and W layers. Each single layer forms a two-dimensional hexagonal lattice. Three of such layers, one W and two Se layers, build Se-W-Se sandwich layers. In each sandwich layer, the Se atoms of the two Se layers reside on top of each other while the W atoms between these two Se layers are positioned in every second empty site of the two-dimensional hexagonal Se lattice (cf. Fig. 1). Therefore, the tungsten atoms have a trigonal prismatic coordination with regard to selenium. The parallel position of one sandwich layer relative to the next determines the vertical size of the bulk unit cell, which contains two sandwich layers in the case of WSe_2. In this unit cell, the W atoms of one sandwich layer reside on top of the Se atoms of the next layer and vice versa. Hence, the stacking order of the two-dimensional hexagonal lattices is *-ABA-BAB-* (cf. Fig. 1). The space group of the structure, which is called $2H_b$, is the non symmorphous D_{6h}^4 or $P6_3/mmc$, respectively. The corresponding Brillouin zone together with the irreducible part and the high-symmetry points is shown in Fig. 2. The experimentally determined[18,19,9] values of the lattice parameters for *a* range from 3.280 to 3.286 Å and for *c* from 12.950 to 12.976 Å. The half diameter of the sandwich layer has been measured[18] as $z = 0.129 \cdot c$, resulting in *z* values from 1.671 to 1.674 Å. The distance between the sandwich layers $w = c/2 - 2z$ is therefore, found in the range from 3.133 to 3.140 Å.

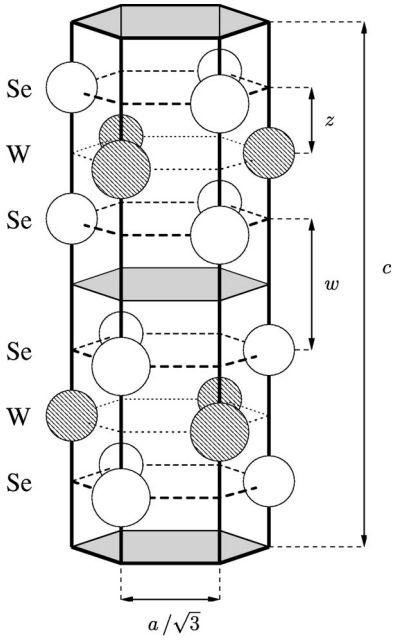

FIG. 1. Crystal structure of WSe_2. The structure parameters *z* and *w* are indicated, as well.

A. Structural and electronic properties of bulk WSe_2

1. Structural properties of WSe_2

The optimization of the bulk crystal structure is done by total energy minimization with respect to the lattice param-

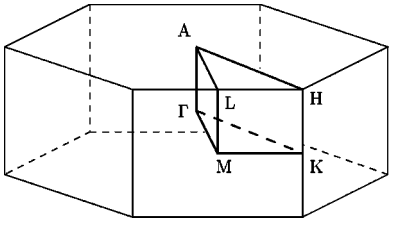

FIG. 2. Bulk Brillouin zone together with the irreducible part.

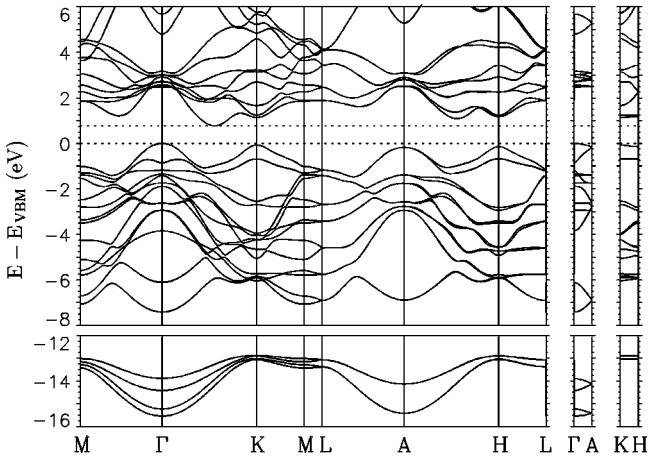

FIG. 3. Bulk band structure of WSe_2 for the theoretical lattice constants. Note that the band structure shows an indirect gap.

eters a and c, as well as, to the half diameter of the sandwich layer z. Using pseudopotentials in the fully separable form of Ref. 14 and neglecting spin-orbit interaction, we obtain $a=3.285$, $c=12.748$, and $z=1.678$ Å, which is $0.132\cdot c$. This gives an intersandwich layer distance w of 3.018 Å. Including spin-orbit interaction in our calculations, yields structure parameters within 0.3 to 0.7 % of the former results. Since inclusion of the latter leads to small deviations only, we neglect the numerically very time consuming incorporation of the spin-orbit interaction for the structure optimizations presented in this paper. In both cases, the differences between our theoretically determined lattice parameters and the experimental values are small. The deviations are in the order of 1% for a, 3% for c, and 1% for z, resulting in a deviation of about 4% for w. Likewise, using the pseudopotentials of Ref. 13 in the nonseparable form in our calculations, yields structure parameters, which differ up to 2% from the results mentioned above, as well.

The relatively large difference between the measured and calculated values of w and c, respectively, may be related to an insufficient description of the long-range interactions between the sandwich layers within the local density approximation.[19]

2. Electronic properties of WSe_2

The experimental and theoretical lattice parameters are almost the same, as discussed above. Therefore, we only show in Fig. 3 the bulk band structure of WSe_2 as resulting for the theoretical lattice parameters.

The electronic configuration of the Se atoms is $[\mathrm{Ar}]3d^{10}4s^24p^4$ and that of the W atoms is $[\mathrm{Xe}]4f^{14}5d^46s^2$. In consequence there is a fairly strong $p-d$ interaction between the W and the Se layers within each sandwich layer, while the interaction between neighboring sandwich layers is only weak and of van der Waals type. While the lowest valence bands at -14 eV exhibit strong Se4s character, the valence bands above -8 eV, as well as, the lower conduction bands originate mainly from hybridized Se4$p-$W 5d states.

We do not address each particular band of these band structures in great detail but rather focus on a few salient features. The upper valence bands have a width of 7.42 eV when the theoretical and 7.19 eV when the experimental lattice constants are used in the calculations. The calculated optical gap energy is 0.77 and 0.86 eV, respectively, in the two cases. Thus, the well-known underestimate of the gap energy within LDA amounts to 39% and 32%, respectively. The experimental band gap energy is about 1.2 eV.[20] The conduction-band minimum (CBM) results from both calculations at 55% of the Γ-K distance, which happens to coincide with the measured value.[11] The valence-band maximum results in the center of the Brillouin zone at the Γ point in both cases using the theoretical, as well as, the experimental structure parameters. The difference between the energy values of the topmost valence band at the Γ and the K point is about 32 meV larger when we employ the theoretically optimized structure parameters, as compared to the calculation employing the experimental structure.

TABLE I. Measured $\Delta E=E_{vb}^{\max}(\Gamma)-E_{vb}^{\max}(K)$ values as resulting from various experiments.

Method	VBM	ΔE (meV)	Ref.
ARPES	Γ	400	21
ARPES	Γ	30	11
ARPES	K	-80	9

Let us look at the two most prominent uppermost valence bands in some more detail (see Fig. 3), as they result from our fully relativistic calculations. As the main effect of the inclusion of spin-orbit interaction, we observe a removal of the degeneracy of these bands along A-H-L, which obtains if spin-orbit interaction is neglected. In contrast, a splitting along Γ-K-M is observed even without including spin-orbit interaction. At the K point, these upper two valence bands exhibit mainly metal $d_{xy}/d_{x^2-y^2}$ (about 76%) and chalcogen p_x/p_y (about 23%) character. Therefore, the respective states originating from the $p-d$ hybridization are directed parallel to the sandwich layers. From K to H, i.e., perpendicular to the layers, this characteristics does not change very much. Therefore, the two uppermost valence bands show only a weak dispersion along K-H (about 0.1 eV for the upper band). On the other hand, the dispersion perpendicular to the layers of the topmost valence band at Γ, which exhibits mainly metal d_{z^2} (about 67%) and chalcogen p_z (about 21%) character, is twice as large. For the second topmost valence band (about 98% Se p_z) the dispersion along Γ-A is with 0.8 eV even larger indicating the interaction between the sandwich layers.

An overview on the results of experimental and theoretical investigations determining the position of the VBM in the Brillouin zone is given in Tables I and II, respectively. Two positions in **k** space, one at Γ and the other at K, are favored as VBM by these studies. To ease the comparison of the results from the literature and from our calculations, we define the quantity ΔE as the energy difference between the highest occupied valence band at Γ and at K as

$$\Delta E=E_{vb}^{max}(\Gamma)-E_{vb}^{max}(K). \tag{1}$$

Within this definition, a positive value of ΔE indicates that the VBM is at Γ, and a negative value means that the VBM is at K. In Table II we have labeled the different results of the

TABLE II. $\Delta E = E_{vb}^{\max}(\Gamma) - E_{vb}^{\max}(K)$ values as resulting from various LDA calculations.

Method	Spin-orbit	VBM	ΔE (meV)	z/c	Ref.
ASW[a]	No	Γ	500	0.121	18
LAPW	Yes	Γ	98	0.129[c]	10
LAPW	Yes	Γ	41	0.131[d]	10
RLMTO	Yes	K	-18	0.125	11
ELAPW	no	Γ	224	0.125	11
PPGO[b]	Yes	Γ	39	0.129[c]	This work
PPGO	Yes	Γ	71	0.132[e]	This work
PPGO	No	Γ	173	0.132[e]	This work

[a]Augmented spherical wave (ASW) method.
[b]Pseudopotential calculation with Gaussian orbitals (PPGO) basis set.
[c]Experimental lattice parameter.
[d]Parameter z optimized with a and c at their experimental values.
[e]Theoretical lattice parameter.

various calculations by the method used for the calculations, the geometry used, i.e., theoretical or experimental lattice parameters, and whether they have been carried out with or without spin-orbit interaction. The comparison of the theoretical results from the literature (see the first five lines in Table II), shows that most of these calculations have employed different crystal parameters a, c, and especially z. Furthermore, some of these calculations have neglected the spin-orbit interaction. In addition, the different calculations have been based on different methods. Thus, a direct comparison of these results is not straightforward at all. Differences in the results can very well be due to differences in the methodology used.

To clearly identify the influence of the structure parameters used in the calculations and the effects of including or neglecting spin-orbit interaction on ΔE, we have analyzed these different cases on equal footing within the framework of one and the same method. The results are shown in the lower part of Table II. Our investigations using the theoretically optimized crystal structure yield a difference of $\Delta E = 102$ meV between the calculation with and without spin-orbit interaction taken into account. However, the valence-band maximum is at Γ in both cases. Including spin-orbit interaction and employing the experimental lattice structure, the difference in energy ΔE of the topmost band at Γ and K decreases to only 39 meV, which is in excellent agreement with the experimental value of 30 meV found by Traving *et al.*[11] In Table II, we see a sensitive dependence of ΔE on the ratio z/c and on spin-orbit interaction.

We have, therefore, studied the dependence of ΔE and of the energy of the indirect optical gap E_g on z and w, i.e., on half the sandwich layer thickness and the separation between the sandwich layers. With increasing z for fixed a and w, as well as, with increasing w for fixed a and z, these quantities show significant changes. The results are plotted in Figs. 4 and 5. These calculations were carried out at the experimental values of a and w or z, respectively. The plots show an almost linear dependence of ΔE as a function of z and w. With increasing values, in both cases, the position of the VBM in **k** space changes from Γ to K for slightly higher values than the experimental ones. The change of the gap

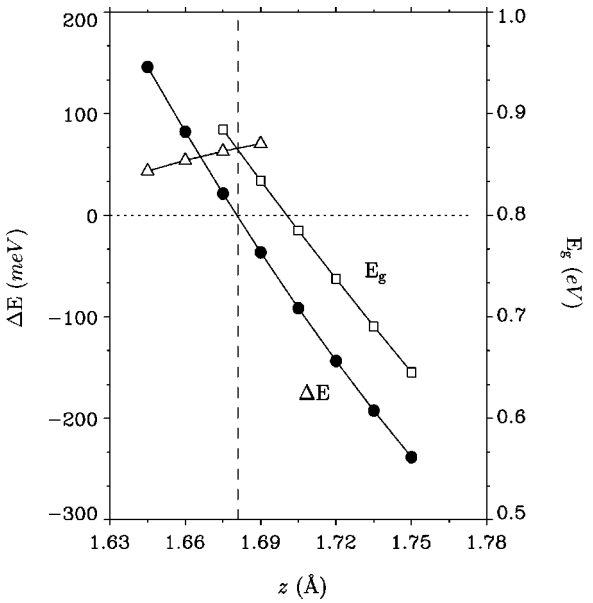

FIG. 4. $\Delta E = E_{vb}^{\max}(\Gamma) - E_{vb}^{\max}(K)$ (left axis, filled circles) and gap energy (right axis) between Γ and the CBM (triangles) and between K and the CBM (squares) for fixed a and w values as a function of the sandwich layer thickness z.

energy as a function of z or w also marks this transition in **k** space. With increasing sandwich layer thickness $2z$ for a fixed value of w, we observe for small z a slowly increasing gap energy, defined by the indirect gap between Γ and the CBM. After the VBM changes to the K point the gap is defined by the indirect gap between K and the CBM. It decreases with approximately the same rate as ΔE, because of an almost constant gap between the topmost valence band at Γ and the CBM. On the other hand, with increasing distance of the sandwich layers w, the indirect gap increases also.

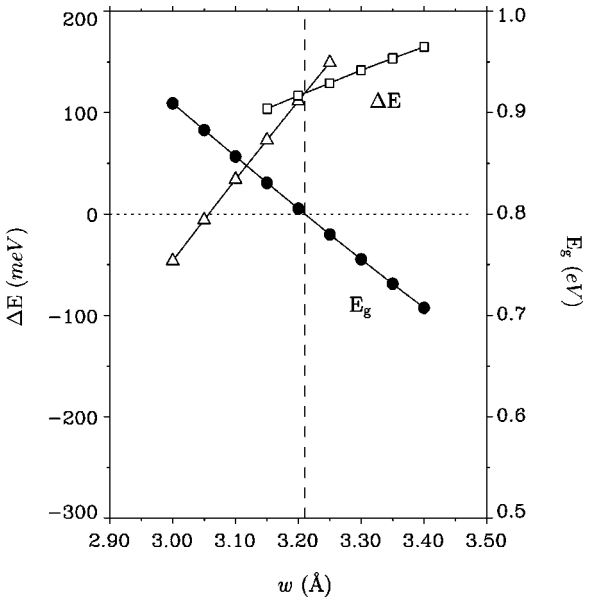

FIG. 5. $\Delta E = E_{vb}^{\max}(\Gamma) - E_{vb}^{\max}(K)$ (left axis, filled circles) and gap energy (right axis) between Γ and the CBM (triangles) and between K and the CBM (squares) for fixed a and z values as a function of the distance w between the sandwich layers.

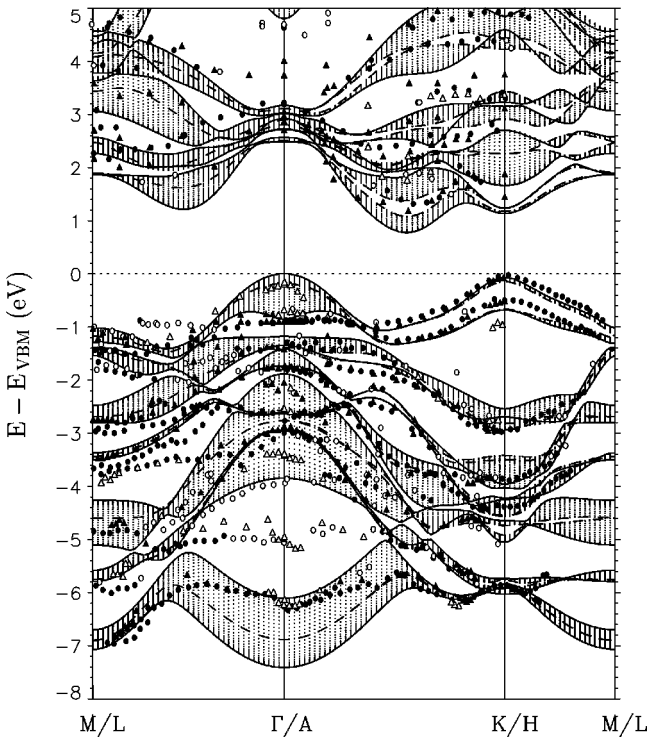

FIG. 6. Experimental band structure of Finteis *et al.* (Ref. 9) and of Traving *et al.* (Ref. 11) (circles and triangles, respectively; open symbols denote weak and full symbols denote pronounced structures) in comparison with the PBS (point pattern) and the bulk band structure for $k_\perp = 0$ (solid lines) and $k_\perp = \pi/c$ (dashed lines).

Indeed, we observe a much larger gap (see below) for a WSe_2 film of one sandwich layer, for which no interaction with other layers exists at all.

In Fig. 6, the bulk band structure of WSe_2, projected[22] onto the $\mathbf{k}_\parallel$ plane in the bulk Brillouin zone, is shown together with experimentally determined band energies. This calculation has been carried out for the optimized structural parameters. We use the projected band structure (PBS) of the bulk crystal for comparison, since the available experimental ARPES and ARIPES data are not resolved with respect to $k_\perp$. We show in Fig. 6 bands along M-Γ-K and L-A-H as solid or dashed lines, respectively. The data points show ARPES and ARIPES results from Finteis *et al.*[9] and from combined photoemission and inverse photoemission experiments of Traving *et al.*[11]

The two experimental data sets are in excellent mutual agreement. Only for the observed conduction bands there are small deviations. Comparing the data with our theoretical results, we find a very good agreement between measured and calculated valence bands both with respect to their dispersion, as well as, to their absolute energy position. This is quite obvious, in particular, for sections of the valence bands that exhibit only a marginal dispersion in the $k_\perp$ direction (see, for instance, most of the valence bands near the K point). A marked exception from this good correspondence between our theoretical results and the data is most obvious in the projected energy gap at around -5 eV near the Γ point. The measured band is almost dispersionless and there is no counterpart for it in our theoretical results. The same obtains for the observed band near -4 eV at M/L, which shows a more pronounced dispersion from M to Γ. These differences between the observed data and the theoretical band structures hold for the results of our, as well as, of all other calculations[8–11] mentioned above.

The comparison between our results and the experimental data shows, in addition, very clearly the importance of the spin-orbit coupling for a correct description of the bands. Without spin-orbit interaction, the two uppermost valence bands at the H point coincide. In this case, the gap between the topmost bands at K/H in the PBS closes. In experiment, a splitting of about 0.5 eV at the topmost lines at K/H is observed. The results of our calculation are in very good agreement with this finding. The same holds for the dispersion of these bands along Γ-K-M.

The calculated conduction bands show an almost constant shift of about 0.3 eV to lower energies with respect to the experimental bands. This is a typical consequence of the LDA underestimate of band gap energies. Except for this rigid shift, the calculated bands are in good accord with the experimental data.

Summarizing this part of the discussion, our calculated band structure of WSe_2 is in gratifying agreement with the observed photoemission and inverse photoemission results of Finteis *et al.*[9] and Traving *et al.*,[11] respectively. Concerning the position of the VBM, we have shown that only small changes of the distance between the sandwich layers or of their thickness influence the position of the VBM drastically. Therefore, sample preparation is a very important issue in this problem. Furthermore, in our opinion a satisfactory theoretical determination of the electronic structure of WSe_2 in the gap energy region with an accuracy of better than a few tenths of an eV is at least questionable within LDA because of the inherent inaccuracy of the description of long-range correlations. The latter, however, can be expected to be important for WSe_2 because of the van der Waals interactions between neighboring sandwich layers. This is a common problem of all LDA calculations of WSe_2 cited in this paper.

Deviations between experiment and theory, and in particular the **k**-space position of the VBM have been suspected by Finteis *et al.*[10] to be related to the influence of surface effects. This expectation, however, is not warranted by our results for thin WSe_2 films, to be discussed in the next subsection.

B. Structural and electronic properties of WSe_2 films

We have determined electronic and structural properties of thin WSe_2 films employing the well-known supercell method. We have used systems with vacuum regions with a thickness of one or three sandwich layers, which translates into distances between two material films of 9.6 and 22.6 Å, respectively. Both yield nearly identical results. This shows that a vacuum region with a thickness of one sandwich layer is sufficient for good convergence. To study the dependence of the structural parameters on the thickness of the films (i.e., the number of sandwich layers) we have explicitly calculated the *structure* of films with one up to five WSe_2 sandwich layers in the supercell by energy minimization with respect to the distance between the sandwich layers and their thickness. In addition, we have also calculated the lattice parameter a for the single sandwich layer. The resulting parameters in all cases do not differ by more than 0.2% from the values

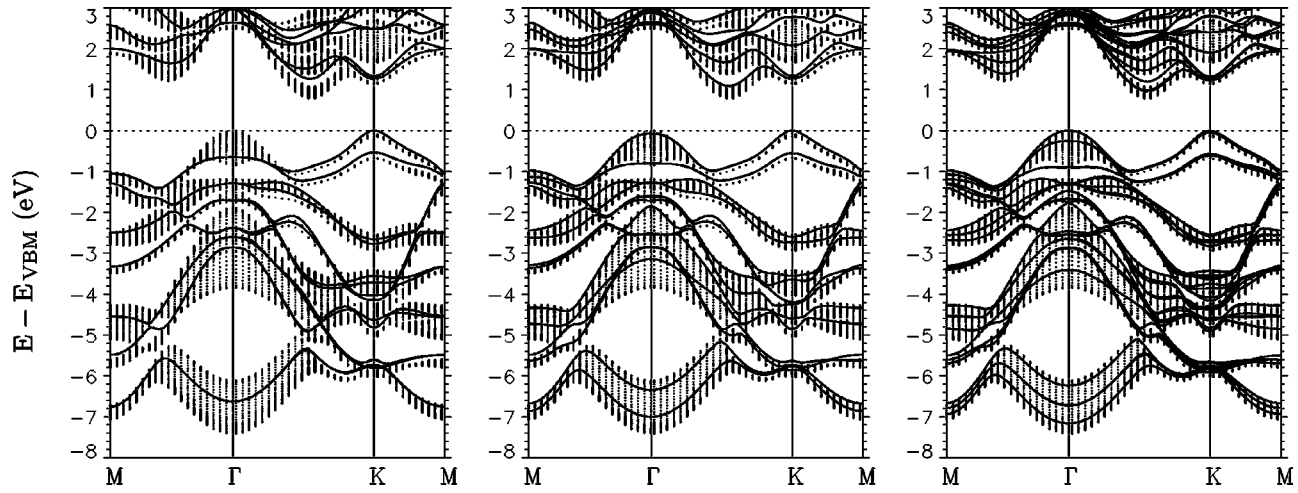

FIG. 7. Calculated band structure of thin WSe_2 films with 1, 2, and 3 sandwich layers (full lines) in comparison with the projected bulk band structure (point pattern).

of the optimized bulk structure. Thus, we find no relaxation of the sandwich layers. Combining single sandwich layers to a bulk crystal yields an energy gain of 17 meV per unit cell, only. This result and the lack of relaxation in the supercell, as discussed above, allow to rationalize the two-dimensional character of the layered WSe_2.

Concerning the *electronic structure* we have studied the transition from a single sandwich layer per supercell up to bulk WSe_2 films by carrying out calculations for one up to five sandwich layers in the supercell. In all of these calculations we have taken spin-orbit interaction into account. The experimental lattice parameters *a* and *z* of the bulk have been used in these calculations. In Fig. 7, we show the band structures of the one-, two-, and three-sandwich layer films. In order to be able to resolve surface states or resonances, we show the PBS of the bulk[22] as a reference.

By looking at the uppermost part of the valence bands in the PBS around the Γ point, we observe one, two, and three bands for the calculations with one, two, and three layers in the supercell, respectively. The same behavior is most obvious for the bands around -6.5 eV. Interestingly enough, the three bands near the Γ point around -1.0 and -6.5 eV span almost the full energy range of the underlying PBS.

Comparing the supercell bands with the PBS of the bulk crystal (see Fig. 7), we observe that none of the bands of the thin films shows any clearly resolvable surface state in the fundamental group. This again highlights the two-dimensional character and the weak coupling of the sandwich layers in WSe_2 by van der Waals interaction. For the one layer sandwich the VBM and the CBM are both localized at the *K* point of the surface Brillouin zone so that this system has a direct gap. The gap energy of this one sandwich layer system is 0.5 eV larger than that of the fundamental bulk gap. An increase of the film size leads to an increased number of bands that are filling the projected bulk band region. Likewise, ΔE and the size of the gap decrease as can be seen in Table III.

While the band dispersion of the two sandwich layer film is already roughly the same as for the bulk, only the films of three and more sandwich layers also exhibit the same VBM position, i.e., at Γ. The change in the position of the VBM results from the different character of the topmost bands at *K* and Γ. The orbitals contributing to the highest occupied band at the *K* point are directed parallel to the surface and, therefore, the dispersion of these bands is almost independent of the thickness of the film. On the other hand, the orbitals constituting the highest occupied band at Γ are directed perpendicular to the surface. Therefore, the corresponding states are influenced more significantly by the interaction between different sandwich layers. An increase of the film thickness thus leads to a remarkable change in the energy positions and dispersion of these bands. This is obvious for the position of the topmost valence bands at Γ of one sandwich layer film in contrast to the other films and the bulk crystal. In the first case, the bands lie more than 0.6 eV below the bulk VBM, in the latter case they are split in several bands with the top band almost coinciding with the bulk VBM.

To further clarify the changes of the electronic structure as a function of film thickness, we compare our results for the one and the two sandwich layer films in some more detail. At the Γ point, a Mulliken analysis for the one sandwich layer shows that the topmost, degenerate band at about 0.6 eV below the bulk VBM consists mainly of $W\,5d_{z^2}$ orbitals (62%) and to a smaller extent of $Se\,4p_z$ (14%) orbitals. Therefore, the respective states are perpendicular to the surface layers. When a second sandwich layer is added to form the two sandwich layer film, this band splits into two bands at Γ, caused by the interaction between the two layers. In this case the $W\,5d_{z^2}$ orbital contribution is about 30% per each tungsten layer (this is obvious from symmetry), but the orbital contributions from the Se layers are different for the two bands. The two Se layers localized between the two W

TABLE III. $\Delta E = E_{vb}^{\max}(\Gamma) - E_{vb}^{\max}(K)$ and the gap energy for the films and the bulk.

Sandwiches	VBM	ΔE (meV)	Gap (eV)
1	*K*	−642	1.27
2	*K*	−65	1.06
3	Γ	2	0.96
5	Γ	48	0.85
∞	Γ	71	0.77

layers, i.e., in the middle of the two sandwich layers, contribute 16% each to the upper band (the two other Se layers 2% each). These contributions mainly originate from Se $4p_z$ orbitals. For the lower band, on the contrary, the orbitals on the Se layers above and below the film are involved with about 12% of their wave-function amplitudes, while the ones in the middle contribute less than 5%. Thus, the interaction between the sandwich layers splits the bands and shifts the upper one towards the VBM. A similar band splitting is observed for the lowest band near -6.5 eV at the Γ point. Here the bands consist of W $6s$ and W $5d_{z^2}$ (26% and 23%, respectively) and Se $4p_{z^2}$ (44%) orbitals for the film of one sandwich layer.

From all of our results, we infer, that the sensitive dependence of the relative energy positions of the Γ and K points is mostly due to the sensitivity of states near Γ on lattice parameters (see Figs. 5 and 7).

IV. SUMMARY

We have reported *ab initio* calculations of the geometric and the electronic structure of thin films, as well as, of bulk WSe_2, as a prototype for layered VIb transition-metal dichalcogenides. For the bulk crystal, our results show a strong dependence of the position of the VBM on the distance and the thickness of the two sandwich layers within the unit cell. Using our optimized or the experimental crystal structure we find the valence-band maximum at the Γ point. Our theoretical band-structure results show a very good overall agreement with ARPES and ARIPES data. Contrary to our findings for the bulk crystal, for thin films with one or two sandwich layers we find the VBM at the K point. On the other hand, for slightly different crystal parameters we observe the VBM for the bulk at the K point, as well. We therefore believe that the conflicting results in the experimentally determined position of the VBM could originate from specific conditions in crystal growth. The intercalation of atoms, e.g., of the used transport gas in the growth of the sample could give rise to different positions of the VBM, because a small change in the separation of the sandwich layers or their thickness would yield a different VBM position.

ACKNOWLEDGMENTS

It is our great pleasure to thank Dr. Klaus Würde for fruitful discussions and for his help and support to include the spin-orbit interaction in our calculations.

[1] H. Fuchs and Th. Schimmel, Adv. Mater. **3**, 112 (1991).
[2] Th. Schimmel, H. Fuchs, S. Akari, and K. Dransfeld, Appl. Phys. Lett. **58**, 1041 (1991).
[3] Th. Schimmel, R. Kemnitzer, J. Küppers, H. Fuchs, and M. Lux-Steiner, Thin Solid Films **254**, 147 (1995).
[4] A. Asenjo, T. Schwaack, P. de Pablo, J. Gómez-Herrero, E.K. Schweizer, C. Pettenkofer, H. Fuchs, and A. M. Baró, Surf. Sci. **398**, 231 (1998).
[5] H. Tributsch, J. Electrochem. Soc. **125**, 1086 (1978).
[6] H. J. Lewerenz, A. Heller, and F. J. DiSalvo, J. Am. Chem. Soc. **102**, 1877 (1980).
[7] G. Prasad and O. N. Srivastava, J. Phys. D **21**, 1028 (1988).
[8] Th. Straub, K. Fauth, Th. Finteis, M. Hengsberger, R. Claessen, P. Steiner, S. Hüfner, and P. Blaha, Phys. Rev. B **53**, R16 152 (1996).
[9] Th. Finteis, M. Hengsberger, Th. Straub, K. Fauth, R. Claessen, P. Auer, P. Steiner, S. Hüfner, P. Blaha, M. Vögt, M. Lux-Steiner, and E. Bucher, Phys. Rev. B **55**, 10 400 (1997).
[10] Th. Finteis, M. Hengsberger, Th. Straub, K. Fauth, R. Claessen, P. Auer, P. Steiner, S. Hüfner, P. Blaha, M. Vögt, M. Lux-Steiner, and E. Bucher, Phys. Rev. B **59**, 2461 (1999).
[11] M. Traving, M. Boehme, L. Kipp, M. Skibowski, F. Starrost, E.E. Krasovskii, A. Perlov, and W. Schattke, Phys. Rev. B **55**, 10 392 (1997).
[12] P. Hohenberg and W. Kohn, Phys. Rev. **136**, B864 (1964).
[13] G. B. Bachelet, D. R. Hamann, and M. Schlüter, Phys. Rev. B **26**, 4199 (1982).
[14] X. Gonze, R. Stumpf, and M. Scheffler, Phys. Rev. B **44**, 8503 (1991).
[15] L. Kleinman and D. M. Bylander, Phys. Rev. Lett. **48**, 1425 (1982).
[16] D. M. Ceperley and B. J. Alder, Phys. Rev. Lett. **45**, 566 (1980).
[17] J. P. Perdew and A. Zunger, Phys. Rev. B **23**, 5048 (1981).
[18] R. Coehoorn, C. Haas, J. Dijkstra, C. J. F. Flipse, R. A. de Groot, and A. Wold, Phys. Rev. B **35**, 6195 (1987).
[19] R. Manzke and M. Skibowski, in *Electronic Structure of Solids: Photoemission Spectra and Related Data*, edited by A. Goldmann, Landolt-Börnstein, Group III, Vol. 23, Pt. b (Springer-Verlag, Berlin, 1994), p. 84.
[20] Kam-Keung Kam, Chi-Lan Chang, and D. W. Lynch, J. Phys. C **17**, 4031 (1984).
[21] R. Coehoorn, C. Haas, and R. A. de Groot, Phys. Rev. B **35**, 6203 (1987).
[22] In detail, we have plotted several band structures at $k_\perp = \text{const}$ for an equally spaced $k_\perp$ mesh.